

Alkali-metal adsorption on dissimilar alkali-metal monolayers preadsorbed on Cu(001): Li on Na and Na on Li

Seigi Mizuno and Hiroshi Tochiwara*

Catalysis Research Center, Hokkaido University, Kita-ku, Sapporo 060, Japan

Takaaki Kawamura

Department of Physics, Yamanashi University, Kofu, Yamanashi 400, Japan

(Received 29 March 1994; revised manuscript received 8 August 1994)

An adsorption system of metal-on-metal growth is presented. The adsorption of alkali-metal atoms on monolayers of dissimilar alkali metals preadsorbed on the Cu(001) surface has been studied by Auger-electron spectroscopy, work-function change, and low-energy electron-diffraction intensity analysis. We have examined the following three adsorption systems on Cu(001) at 180 K: Na on a full monolayer of Li, Li on a full monolayer of Na, and Na on a submonolayer of Li, namely, the $c(2 \times 2)$ structure of Li adatoms. It is found that a simple overlayer formation of Na takes place on the full Li monolayer, while Li atoms substitute Na adatoms for Li adsorption on the full Na monolayer. For adsorption of Na on the Li- $c(2 \times 2)$ structure whose coverage is $\frac{5}{8}$ of the full Li monolayer, it is found that Na atoms compress the Li adlayer to become denser monolayers. The Na atoms do not intermix with Li adatoms, but they form islands of the $c(2 \times 2)$ structure on Cu(001).

I. INTRODUCTION

The adsorption of alkali-metal atoms on transition- or noble-metal surfaces has been studied experimentally and theoretically for many years.¹ One of the most interesting features of alkali-metal adsorption on the metals is drastic changes of surface structures and properties during monolayer formation, typically seen in the work-function change.¹ In these changes we have an implicit understanding that alkali-metal atoms form overlayers on metals. Recent studies, however, have revealed that reconstructions of the substrate take place on some metal planes upon alkali-metal adsorption at room temperature. For example, on fcc(110) metal surfaces of Ag, Cu, Ni, and Pd, it is known that alkali-metal atoms induce a missing-row-type reconstruction of substrate surfaces at 300 K.² On fcc(001) also, missing-row-type reconstructions in the top layer are found for K/Ag(001),³ K/Au(001),⁴ and Li/Cu(001) (Ref. 5) at 300 K. Even on fcc(111), a substituted top substrate layer of the $(\sqrt{3} \times \sqrt{3})R30^\circ$ structure is determined for K/Al(111) by low-energy electron-diffraction (LEED) analysis.⁶ Following the missing-row-type reconstruction or substitutional adsorption, surface alloy formation between substrate and alkali-metal atoms takes place with an increase of coverage for the adsorption systems above. It is noted that temperature necessary for these processes is higher than ~ 200 K.²⁻⁶ On the other hand, at temperatures lower than 200 K, alkali-metal overlayers are formed instead.

As mentioned above, on some transition- and noble-metal surfaces, a variety of growth modes of alkali-metal atoms has been found. It is interesting to use an alkali metal as a substrate to be adsorbed by dissimilar alkali-metal atoms. Since the adsorbate and substrate belong to an alkali-metal group, interaction between them would be

very different from that between an alkali metal and transition or noble metals. Consequently, we may find a type of growth mode different from those already known.

However, it is difficult to make single crystals of alkali metals. Therefore, instead of a bulk crystal, we use a monolayer of alkali metal on Cu(001). Fortunately, monolayers of alkali metals on Cu(001) exhibit well-ordered two-dimensional lattices at low temperatures.⁷⁻¹¹ Therefore, we can study structures and growth modes due to alkali-metal adsorption on dissimilar alkali-metal monolayers by using LEED. To date, this adsorption system, i.e., alkali metal on alkali metal, has not been performed as far as we know.

In this paper, we have studied the following three adsorption systems at 180 K: (1) Na on a full monolayer of Li on Cu(001), (2) Li on a full monolayer of Na on Cu(001), and (3) Na on a submonolayer of Li on Cu(001). In the three adsorption systems, we have found (1) simple overlayer formation of Na, (2) substitution of the Na adatom by Li, and (3) compression of the Li adlayer and phase separation into Li and Na domains, respectively. Following Sec. II (experiment and calculation), detailed results of the three adsorption systems above studied by LEED, Auger-electron spectroscopy (AES), and work-function change are described in Sec. III with some discussion. Summaries are reviewed in Sec. IV.

II. EXPERIMENT AND CALCULATION

Experiments were carried out in a three-level UHV chamber equipped with various probes.¹² LEED and AES were principal tools in the present study. In particular, AES of Li KVV and Na LVV transitions played a crucial role in alkali-metal on alkali-metal systems. The work-function change was measured by using a derivative mode of the AES system, and the cutoff of secondary

electron emission was used with sample bias. The Cu(001) surface was cleaned with a procedure mentioned below. LEED spots from the clean surface were sharp, and the background was satisfactorily low. Alkali metals were deposited onto the surface from SAES dispensers (SAES Getters) at 180 K. LEED spot intensities were measured with a computer-controlled auto-LEED system for surface-structure determination. LEED intensity-energy curves $I(E)$ were taken with an incident-energy range from 20 to 200 eV and with 1-eV steps. The normal-incidence condition was achieved approximately by using the horizontal-beam method,¹³ in which only two equivalent spots located in the horizontal direction are averaged. It should be noted that all experiments were carried out at 180 K. In the present paper, the coverage of alkali-metal atoms is always defined as the ratio of the number density of alkali-metal atoms with respect to that of copper atoms in the ideal Cu(001) surface.

Special care was taken in the present experiment for the following two points. First, we paid attention to pressure in the chamber, because alkali-metal-deposited Cu(001) surfaces are easily contaminated by residual gases. Since water in the chamber is the most active species for alkali-metal-covered Cu surfaces,^{12,14} a liquid-nitrogen shroud was used to remove the water. Then the partial pressure of water was less than 3×10^{-12} Torr during experiments. The total and CO partial pressures during experiments were 1.0×10^{-10} and 3×10^{-12} Torr, respectively. Most of the residual gas was hydrogen, and oxygen was not found. We confirmed by using high-resolution electron-energy-loss spectroscopy (HREELS) that hydrogen is not adsorbed on alkali-metal-deposited Cu(001) surfaces at 180 K. During alkali-metal deposition the pressure rose to 1.5×10^{-10} Torr, and the pressure rise was due to hydrogen with a small increase of CO. After an experiment of alkali-metal adsorption on a dissimilar alkali-metal monolayer, we did not detect hydroxide, oxide, CO or other contaminants by HREELS, AES, x-ray photoelectron spectroscopy, ultraviolet photoelectron spectroscopy or work-function change. It is also noted that no residual gas is adsorbed on the clean Cu(001) surface at 180 K. This keeps the surface clean until alkali-metal atoms are deposited.

Second, we paid attention to cleaning of the Li-deposited surface after an experiment, because Li atoms interdiffuse into bulk at high temperatures. The Li-adsorbed surface was first cleaned by Ar-ion sputtering then annealed up to 600°C. With this procedure, we always obtained a clean surface. When we changed the order of sputtering and annealing, we obtained a contaminated surface due to segregated and reacted Li atoms. At room temperature, as shown in our previous studies,⁵ Li atoms replace copper surface atoms and form surface alloys. It was found by using AES and HREELS for electronic excitations that Li atoms stay in the surface region at 300 K. At 180 K, where the experiments were performed, Li atoms do not replace substrate atoms and do not interdiffuse into the bulk.

Standard LEED programs¹⁵ were used to calculate $I(E)$ curves. Six phase shifts were used to calculate

atomic scattering ($I_{\max} = 5$). The real part of the inner potential is determined during the course of the theory-experiment fit. The Debye temperature of Cu is 335 K. The Debye temperatures of the Li and Na overlayers are 480 (Ref. 7) and 160 K,¹⁶ respectively.

III. RESULTS AND DISCUSSION

A. Li or Na-atom adsorption on Cu(001)

Here we briefly summarize structures of Li or Na adsorption on Cu(001) observed with LEED in order to help in understanding results of alkali-metal on alkali-metal systems. In addition, we describe Auger transitions of Li and Na adatoms on copper surfaces, because they play an important role in the alkali-metal on alkali-metal systems as demonstrated in the main part of this paper.

1. LEED observations

In Fig. 1, sequential changes of LEED patterns for Li or Na adsorption on Cu(001) at 180 K are summarized with an increase of coverages. Similar adsorption systems, K (Refs. 8 and 9) or Cs (Refs. 10 and 11) on Cu(001), have been studied previously. The $c(2 \times 2)$ structures, observed for both Li (Ref. 7) and Na (Ref. 16) adsorption systems, have been determined by means of LEED intensity analysis. It was found that Li or Na adatoms occupy the fourfold hollow sites of the Cu(001) surface and that the coverages are 0.5. The Na- $c(2 \times 2)$ structure corresponds to the full monolayer, while the Li- $c(2 \times 2)$ structure is a submonolayer whose coverage is $\frac{5}{8}$ of the full monolayer, as seen in Fig. 1. Complicated structures at high Li coverages are due to overlayers, and we will propose these structure models elsewhere.¹⁷

2. AES of Li KVV and Na LVV

Previously, we found two Auger peaks of Li KVV at 46 and 49 eV for the Li-deposited Cu(001) surfaces.⁵ We deduced that the 49-eV Auger electrons come from Li $2s$ valence electrons in the deexcitation process of a Li $1s$ hole. They are denoted as the Li($1s$)Li($2s$)Li($2s$) transition. On the other hand, the 46-eV Auger electrons were ascribed to an interatomic transition between Li atoms and Cu atoms bonded with the Li atoms. They are

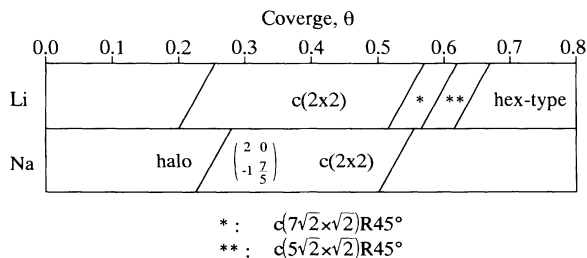


FIG. 1. Surface-structure changes for adsorption systems of Li/Cu(001) and Na/Cu(001) at 180 K as a function of alkali-metal coverage, θ .

denoted as the $\text{Li}(1s)\text{Cu}(3d)\text{Cu}(3d)$ transition; Cu 3d electrons are involved in the deexcitation of a Li 1s hole. Estimated kinetic energies of the two Auger peaks were in good agreement with those of our experiments.⁵ A feature of the Li KVV Auger transitions on copper surfaces is schematically depicted in Fig. 2. In the first monolayer Li adatoms emit both 49- and 46-eV Auger electrons as shown in Fig. 2(a), while Li atoms in the second layer emit only 49-eV Auger electrons as shown in Fig. 2(b). This difference comes from the different deexcitation processes mentioned above. It should be noted that AES of the Li KVV transitions is a powerful tool for studies of Li-atom adsorption on Na atoms preadsorbed on Cu substrate, because we can easily distinguish Li atoms sitting on the copper substrate from Li atoms sitting on Na adatoms by Li KVV Auger electrons. That is, the Li atoms sitting on the copper substrate have two Auger peaks, while Li atoms adsorbed on Na atoms have only one peak.

We have observed a similar doublet peak of LVV Auger electrons of Na adatoms on Cu(001) at 22 and 25 eV to that of the Li KVV Auger electrons at 46 and 49 eV. The appearance of the two Na LVV Auger peaks can be ascribed to a similar mechanism to the case of Li adatoms on Cu(001). In Fig. 3, two deexcitation processes of a Na 2p core hole are illustrated. The 25- and 22-eV peaks are denoted as the $\text{Na}(2p)\text{Na}(3s)\text{Na}(3s)$ and $\text{Na}(2p)\text{Cu}(3d)\text{Cu}(3d)$ transitions, respectively. We estimate kinetic energies of the former and latter Auger electrons to be 25.3 and 21.1 eV, respectively, and these are

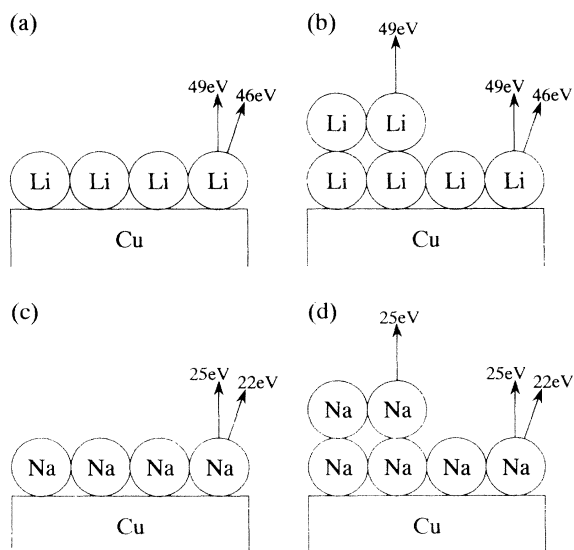


FIG. 2. Illustrations of the characteristic Auger-electron emissions from the first and second layers of Li and Na adatoms on the Cu surface. The Li KVV Auger electrons having kinetic energies of 49 and 46 eV are denoted as the $\text{Li}(1s)\text{Li}(2s)\text{Li}(2s)$ and $\text{Li}(1s)\text{Cu}(3d)\text{Cu}(3d)$ transitions, respectively. The Na LVV Auger electrons at 25 and 22 eV are termed as the $\text{Na}(2p)\text{Na}(3s)\text{Na}(3s)$ and $\text{Na}(2p)\text{Cu}(3d)\text{Cu}(3d)$ transitions, respectively. (a) Li monolayer on copper substrate. (b) Li double layer on Cu. (c) Na monolayer on Cu. (d) Na double layer on Cu.

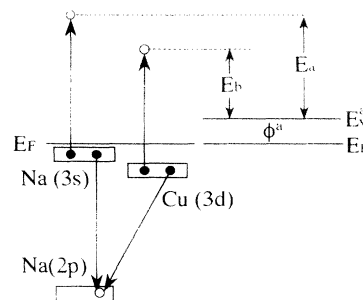


FIG. 3. Schematic diagram for two possible transitions of the Na LVV Auger. E_a and E_b are kinetic energies measured by the analyzer for transitions $\text{Na}(2p)\text{Na}(3s)\text{Na}(3s)$ and $\text{Na}(2p)\text{Cu}(3d)\text{Cu}(3d)$, respectively. E_F is the Fermi level. E_v^a is the vacuum level for the analyzer. ϕ^a is the work function of the analyzer.

in good agreement with our typical peak energies 25.2 and 22.2 eV. As shown in Fig. 2(c), at the first monolayer Na adatoms emit both 25- and 22-eV Auger electrons, while Na atoms in the second layer emit only 25-eV Auger electrons as shown in Fig. 2(d).

B. Na on Li full monolayer

Na atoms are deposited on a full monolayer of Li atoms preadsorbed on Cu(001). The coverage of the Li adatoms is 0.8 at the full monolayer, as mentioned above. Auger spectra in an energy range from 15 to 70 eV for the clean and the full Li monolayer surfaces are shown in Figs. 4(a) and 4(b), respectively. The sensitivity of the detector is changed at an energy of 30 eV. In Fig. 4(a), a doublet peak at 58 and 56 eV is due to MNN Auger electrons of the copper substrate. In Fig. 4(b) a doublet peak at 49 and 46 eV is seen for a full Li monolayer. Figures 4(c) and 4(d) are Auger spectra taken after Na-atom deposition of coverages of 0.07 and 0.25 on the Li monolayer on Cu(001), respectively. In these spectra, a single peak of Na Auger appears at 25 eV. Intensities of both Li Auger peaks decrease when Na atoms are deposited on the Li-covered surface, as clearly seen in Fig. 4(d), and which suggests that the Na atoms cover up the Li monolayer. A clearer evidence for formation of the Na overlayer on the Li-covered surface is that the Na Auger peak at 22 eV does not appear during Na adsorption, as seen in Figs. 4(c) and 4(d). Suppose that Na atoms substitute for Li atoms preadsorbed on Cu(001); then 22-eV Auger peak should be observed, because the Na atoms form bonds with the copper substrate.

Na overlayer formation on the Li full monolayer preadsorbed on Cu(001) is consistent with a result of work-function change measurement. The work-function change is plotted as a function of Li and Na coverages in Fig. 5. In the left-hand-side panel of Fig. 5, a typical work-function change for alkali-metal adsorption systems is observed with increasing Li coverage on Cu(001). The work function reaches a minimum at Li coverage of 0.5 and recovers slightly up to the monolayer completion at coverage of 0.8. The work-function changes at Li cover-

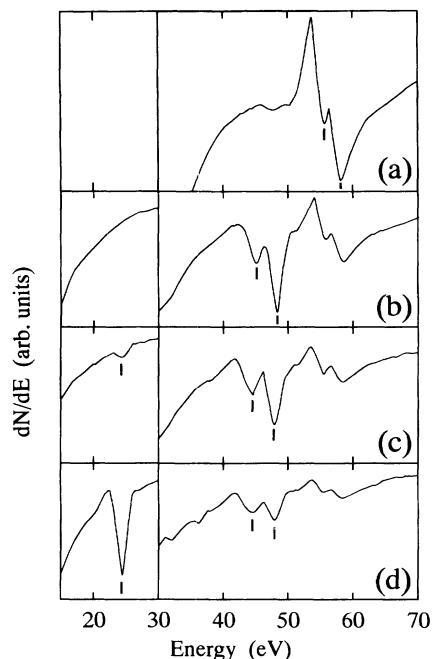


FIG. 4. Na *L**V**V* Auger spectra (left-hand side) and Li *K**V**V* Auger spectra (right-hand side) at 180 K. (a) Clean Cu(001). (b) A full monolayer of Li on Cu(001), $\theta_{\text{Li}}=0.8$. (c) Na is deposited onto the full Li monolayer on Cu(001), $\theta_{\text{Na}}=0.07$. (d) Same as (c), but $\theta_{\text{Na}}=0.25$.

ages of 0.5 and 0.8 are -2.1 and -1.7 eV, respectively. The right-hand-side panel of Fig. 5 depicts the work-function change due to Na deposition on the full Li monolayer on Cu(001). With increasing Na coverage the work function decreases, passes through a shallow minimum, and increases slightly up to a coverage of 0.5 corresponding to a full Na monolayer. At the minimum, where Na coverage is about 0.2, work-function reduction is 0.5 eV from the full Li monolayer. At the end of a monolayer deposition, the work function is estimated to be 2.5 eV from a value of the work function of the Cu(001) surface, 4.6 eV. Reported work functions of bulk

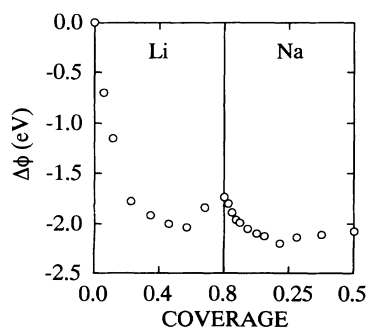


FIG. 5. Work-function change for Li adsorption on Cu(001) at 180 K with increase of Li coverage (left-hand side), and work-function change for adsorption of Na on the full Li monolayer ($\theta_{\text{Li}}=0.8$) at 180 K vs Na coverage (right-hand side).

sodium and lithium metals are 2.4 and 2.9 eV, respectively. Therefore, the result of the work function is consistent with the growth mode that Na adatoms form a monolayer on the full Li monolayer preadsorbed on Cu(001).

C. Li on Na full monolayer

Li atoms are deposited on a full monolayer of Na atoms preadsorbed on Cu(001). The order of deposition of Li and Na is reversed in this case. The Auger spectrum of the starting surface of the full Na monolayer is depicted in Fig. 6(a). Two Na Auger peaks at 25 and 22 eV are observed, and this indicates, of course, that the Na atoms are adsorbed on the copper substrate. Figures 6(b) and 6(c) are Auger spectra taken after Li deposition on the Na monolayer at Li coverages of 0.24 and 1.1, respectively. Two possible growth modes are considered here: overlayer growth and substitutional growth. Suppose that the overlayer growth is the case; only the 49-eV peak of Li Auger should be observed. If substitutional growth occurs, on the other hand, both 46- and 49-eV peaks should be detected. At the same time, the 22-eV peak of Na Auger should disappear with increasing Li deposition. Now we return to Fig. 6(c). In the spectrum two Li Auger peaks appear, whereas a single peak of 25-eV Na Auger is seen. The peak height of the 25-eV Na Auger increases with an increase of Li coverage, as seen in Figs. 6(a)–6(c). These behaviors straightforwardly lead to a conclusion of the substitutional growth of Li on Na. At the monolayer deposition of Li on Na, the top layer consists of Na atoms and the underlying layer consists of Li atoms sandwiched by the Na layer and the Cu(001) surface. Figure 6(c) is very similar to Fig. 4(d), which reflects the fact that the same structure is formed on Cu(001) independently of the order of deposition of Li and Na. The intensity of the 25-eV peak seen in Fig. 6(c) is larger than the summation of the two Na peaks in Fig.

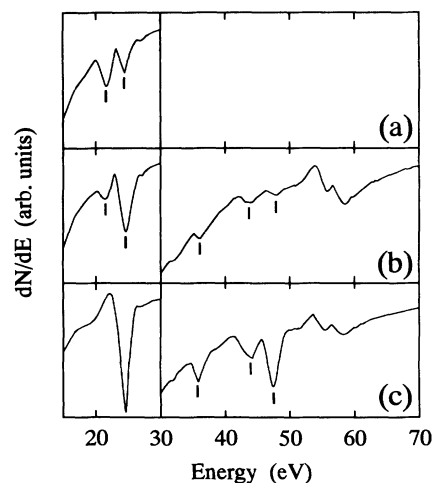


FIG. 6. The Li *K**V**V* and Na *L**V**V* Auger-electron spectra at 180 K. (a) The full Na monolayer on Cu(001), $\theta_{\text{Na}}=0.5$. (b) Li deposited onto the Na full monolayer, $\theta_{\text{Li}}=0.24$. (c) Same as (b) but $\theta_{\text{Li}}=1.1$.

6(a), although the amount of Na atoms does not change. This is an unknown phenomenon of intensity enhancement at the second layer of alkali metals.

In Figs. 6(b) and 6(c), an additional peak appears at 37 eV. The intensity of this peak is proportional to that of the Na 25-eV peak. This has been assigned to the double ionization peak of Na Auger electrons.^{18,19}

Measurements of the work-function change also support the substitutional growth for the adsorption of Li on the full Na monolayer, as shown in Fig. 7. The left-hand-side panel shows the work-function change of the Na-deposited surfaces as a function of Na coverage. At the minimum where Na coverage is about 0.2, the work function is reduced by 2.5 eV. At the full Na monolayer the work function recovers by 0.35 eV and is estimated to be 2.45 eV. These results are similar to the literature.²⁰ Li atoms are deposited on the full Na monolayer, and the change of the work function is plotted in the right-hand-side panel of Fig. 7. It is demonstrated clearly that the work function does not change with an increasing amount of Li adatoms. This suggests that Na atoms are always located in the top layer; each Li atom substitutes for a Na adatom on Cu(001). In fact, the work function of the Li-monolayer-deposited surface on the full Na monolayer (about 2.45 eV) is identical to that of the Na-monolayer-deposited surface on the Li monolayer in Sec. III B (2.5 eV).

We discuss briefly the substitutional absorption. Here we consider two structures on Cu(001): (a) the top Li and underlying Na layers and (b) the top Na and underlying Li layers. We compare total energies $E(a)$ and $E(b)$ for structures (a) and (b), respectively. Binding energies between Li and Na layers can be assumed to be identical for the two structures. Then, the contribution to the total energies are binding energies between the underlying layer and copper substrate, $E(\text{Cu-Li})$ and $E(\text{Cu-Na})$, and surface energies of the top layer, $E(\text{Na})$ and $E(\text{Li})$. To be a stable structure, the surface energy should be small and the binding energy should be large. In thermal desorption spectroscopy from Li or Na-adsorbed Ru(0001) surfaces,^{21,22} we find $E(\text{Cu-Li}) > E(\text{Cu-Na})$. In the literature²³ we find $E(\text{Na}) < E(\text{Li})$. Therefore, this simple argument explains the experimental fact.

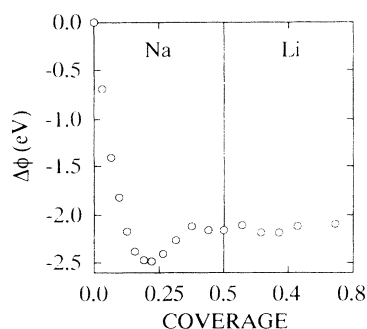


FIG. 7. Work-function change for adsorption Na on Cu(001) at 180 K with increase of Na coverage (left-hand-side panel) and work-function change for adsorption of Li on the full Na monolayer on Cu(001) at 180 K as a function of Li coverage (right-hand-side panel).

D. Na adsorption on $c(2 \times 2)$ structure of Li submonolayer

In this section we investigate the growth mode of Na atoms on a submonolayer of Li atoms preadsorbed on Cu(001), namely the Li- $c(2 \times 2)$ structure. The coverage of the Li- $c(2 \times 2)$ structure is 0.5, while that of the Li full monolayer is 0.8.

1. LEED $I(E)$ curves

We have observed changes of LEED patterns with an increase of Na deposition on the $c(2 \times 2)$ structure of Li atoms preadsorbed on Cu(001). The LEED patterns always exhibit $c(2 \times 2)$ structures up to a Na coverage of 0.5. It is found, however, that the sharpness of half-order spots varies with Na coverage. Initial sharp spots from the Li- $c(2 \times 2)$ structure on Cu(001) become broad up to a Na coverage of 0.1, and finally the spots become sharp again at Na coverages larger than 0.2. This fact suggests that the $c(2 \times 2)$ pattern always observed during Na deposition does not come from a single structure but originates from two structures exhibiting the same $c(2 \times 2)$ pattern. Here it should be noted that both Li and Na adatoms form $c(2 \times 2)$ structures on Cu(001) at a coverage of 0.5, as shown in Fig. 1. Therefore, we have measured $I(E)$ curves of the $(\frac{1}{2}, \frac{1}{2})$ spots as a function of Na coverage, as shown from Figs. 8(a)–8(f). Figure 8(a) is taken from the Li- $c(2 \times 2)$ structure on Cu(001).⁷ For comparison, an $I(E)$ curve of the $(\frac{1}{2}, \frac{1}{2})$ spot of the Na-

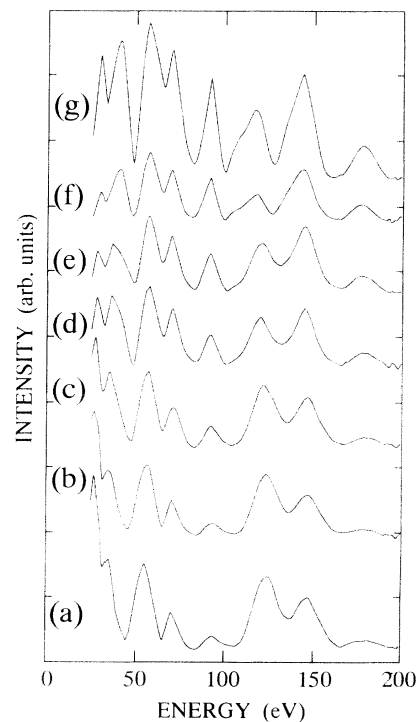


FIG. 8. $I(E)$ curves for the $(\frac{1}{2}, \frac{1}{2})$ spot of the $c(2 \times 2)$ structure formed on Cu(001) at 180 K. (a) The Li- $c(2 \times 2)$ structure on Cu(001). (b)–(f) Na is deposited onto the Li- $c(2 \times 2)/\text{Cu}(001)$. $\theta_{\text{Na}} = 0.05, 0.1, 0.2, 0.3,$ and 0.5 for (b)–(f), respectively. (g) The Na- $c(2 \times 2)$ structure on Cu(001).

$c(2 \times 2)$ structure on Cu(001) is shown in Fig. 8(g).¹⁶ It is evident from Fig. 8 that the $I(E)$ curve changes gradually from that of Li- $c(2 \times 2)$ to that of Na- $c(2 \times 2)$ with increasing Na coverage. We summarize results of LEED $I(E)$ measurements as follows: (i) The Li- $c(2 \times 2)$ structure disappears at Na coverages between 0.1 and 0.2. (ii) The Na- $c(2 \times 2)$ structure is formed on Cu(001) at Na coverages larger than 0.2. Then we propose two possible growth modes for the present adsorption system. First, substitutional growth resulting in formation of the Na- $c(2 \times 2)$ /Cu(001) structure covered with a disordered Li layer, we denote this as the disordered Li top layer on Na- $c(2 \times 2)$ /Cu(001). Second, compression of the Li- $c(2 \times 2)$ structure into a disordered adlayer by Na atoms and formation of the Na- $c(2 \times 2)$ adlayer on vacant copper surface. In the following section, the former is excluded by the analysis of AES.

2. AES of Li KVV and Na LVV

The Auger spectra are taken after Na-atom deposition on the Li- $c(2 \times 2)$ /Cu(001) surface as shown in Fig. 9. Coverages of Na atoms are 0, 0.25, and 0.5 for Figs. 9(a), 9(b), and 9(c), respectively. It is evident from Figs. 9(b) and 9(c) that two Auger peaks appear for both Li and Na atoms. This fact excludes straightforwardly the structure model of the disordered Li top layer on Na- $c(2 \times 2)$ /Cu(001). The other growth model proposed above agrees with the AES result. That is, Na atoms compress the Li adlayer to become a denser monolayer, and the Na atoms do not intermix with Li adatoms and form islands of the Na- $c(2 \times 2)$ structure on Cu(001). The intensity ratio of the Na (22 eV) Auger peak to the Na (25 eV) peak in the present adsorption system seen in Fig. 9(c) is relatively smaller than that of Na adatoms on Cu(001) in Fig. 6(a). This reflects the fact that there are two kinds of Na adatoms in the coadsorption system; one adsorbs onto the Cu surface directly to form the $c(2 \times 2)$

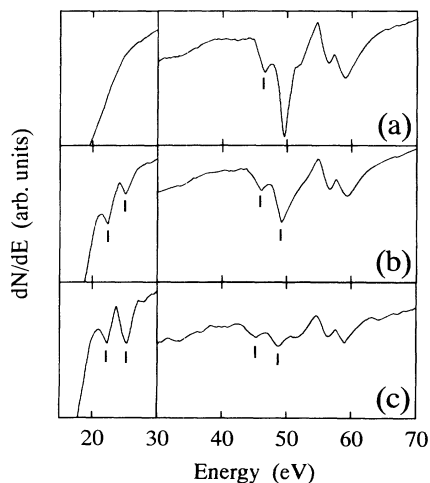


FIG. 9. The Li KVV and Na LVV Auger-electron spectra at 180 K. (a) The Li- $c(2 \times 2)$ structure on Cu(001), $\theta_{\text{Li}}=0.5$. (b) Na is deposited onto the Li- $c(2 \times 2)$ /Cu(001), $\theta_{\text{Na}}=0.25$. (c) Same as (b) but $\theta_{\text{Na}}=0.5$.

structure, and the other adsorbs onto the compressed Li layer or/and on the Na- $c(2 \times 2)$ islands.

3. Growth mode

Why do Na atoms not form an overlayer on the Li- $c(2 \times 2)$ /Cu(001)? If Na atoms occupy the fourfold hollow sites of the Li- $c(2 \times 2)$ structure, the surface also exhibits a $c(2 \times 2)$ order. However, this structure is ruled out by LEED calculation. A reason why Na overlayers do not form on the Li- $c(2 \times 2)$ structure is probably because Li adatoms can be displaced considerably on Cu(001) by a Na atom. As a result, the Na atom can occupy the fourfold hollow sites of Cu(001) and form strong bonds with copper atoms. With an increase of Na deposition, Li adatoms are compressed to be denser layers.

Imagine that the Li- $c(2 \times 2)$ structure is compressed into the densest overlayer of Li adatoms whose coverage is 0.8, then $\frac{3}{8}$ of the Cu(001) surface becomes vacant. Na atoms form the $c(2 \times 2)$ structure on this vacant area up to a Na coverage of $\frac{3}{16}$. After the area is filled with Na atoms up, Na atoms are adsorbed on the Li or Na adlayer randomly. In fact, the $I(E)$ curve of the $(\frac{1}{2}, \frac{1}{2})$ spot does not change in a Na coverage range of $0.2 \leq \theta \leq 0.5$, as seen in Fig. 8. In addition, the intensity of the curve in Fig. 8(f) is smaller than that of the curve Fig. 8(g). These results are in good agreement with that the area of the Na- $c(2 \times 2)$ domains is only $\frac{3}{8}$ of the surface.

The growth mode of the present adsorption system is the compression and phase separation in a coadsorbed layer. This may be one of general phenomena for coadsorption systems. For example, a (2×2) structure of oxygen adsorbed on Pd(111) is compressed into a $(\sqrt{3} \times \sqrt{3})R 30^\circ$ structure with dosing CO which forms $(\sqrt{3} \times \sqrt{3})R 30^\circ$ domains separately.²⁴ At this stage it is not possible to explain the phase separation observed in the present study, but we point out that bulk Li metal does not form an alloy with Na metal.²⁵

IV. SUMMARY

Structure and growth of alkali-metal atoms on dissimilar alkali-metal atoms preadsorbed on Cu(001) has been studied by using AES, LEED, and work-function change. We have studied the following three adsorption systems at 180 K: (1) Na on a full monolayer of Li, (2) Li on a full monolayer of Na, and (3) Na on a submonolayer of Li, namely the Li- $c(2 \times 2)$ structure. The growth modes of these systems are summarized as follows.

(1) Na atoms form overlayers on the full Li monolayer preadsorbed on Cu(001) (overlayer formation).

(2) Li atoms substitute Na adatoms for adsorption of Li on the full Na monolayer preadsorbed on Cu(001) (substitutional adsorption).

(3) For adsorption of Na atoms on the Li- $c(2 \times 2)$ structure whose coverage is $\frac{5}{8}$ of the full Li monolayer, Na atoms compress the Li adlayer to be denser monolayers. The Na atoms do not intermix with Li adatoms and form islands of the $c(2 \times 2)$ structure on Cu(001) (compression and phase separation).

To obtain these conclusion, the Li KVV and Na LVV Auger-electron spectroscopies are very powerful. The

appearance and disappearance of the two Auger peaks of Li and Na adatoms are examined to find growth modes. This is the first successful application of AES of the Li *KVV* and Na *LVV* transitions to surface studies.

ACKNOWLEDGMENTS

Partial financial support from the Iketani Science and Technology Foundation is acknowledged.

*Author to whom all correspondence should be addressed.
FAX: +81-11-709-4748.

¹*Physics and Chemistry of Alkali Metal Adsorption*, edited by H. P. Bonzel, A. M. Bradshaw, and G. Ertl (Elsevier, Amsterdam, 1989).

²R. J. Behm, in *Physics and Chemistry of Alkali Metal Adsorption* (Ref. 1), p. 11; C. J. Barnes, M. Lindroos, D. J. Holmes, and D. A. King, *ibid.* p. 129.

³M. Okada, H. Tochihara, and Y. Murata, *Phys. Rev. B* **43**, 1411 (1991); *Surf. Sci.* **245**, 380 (1991).

⁴M. Okada, H. Iwai, R. Klauser, and Y. Murata, *J. Phys. Condens. Matter* **4**, L593 (1992).

⁵H. Tochihara and S. Mizuno, *Surf. Sci.* **279**, 89 (1992); **287/288**, 423 (1993); S. Mizuno, H. Tochihara, and T. Kawamura, *ibid.* **292**, L811 (1993).

⁶C. Stampfl, M. Scheffler, H. Over, J. Burchhardt, M. Nielsen, D. L. Adams, and W. Moritz, *Phys. Rev. Lett.* **69**, 1532 (1992); C. Stampfl, J. Burchhardt, M. Nielsen, D. L. Adams, M. Scheffler, H. Over, and W. Moritz, *Surf. Sci.* **287/288**, 418 (1993); C. Stampfl, M. Scheffler, H. Over, J. Burchhardt, M. Nielsen, D. L. Adams, and W. Moritz, *Phys. Rev. B* **49**, 4959 (1994).

⁷S. Mizuno, H. Tochihara, and T. Kawamura, *Surf. Sci.* **293**, 239 (1993).

⁸T. Aruga, H. Tochihara, and Y. Murata, *Phys. Rev. Lett.* **52**, 1794 (1984); *Surf. Sci.* **158**, 490 (1985); *Surf. Sci. Lett.* **175**, L725 (1986); *Phys. Rev. B* **34**, 8237 (1986).

⁹H. L. Meyerheim, J. Wever, V. Jahns, W. Moritz, P. J. Eng, and I. K. Robinson, *Surf. Sci.* **304**, 267 (1994).

¹⁰C. A. Papageorgopoulos, *Phys. Rev. B* **25**, 3740 (1982).

¹¹J. Cousty, R. Riwan, and P. Soukiassian, *Surf. Sci.* **152/153**, 297 (1985).

¹²S. Mizuno, H. Tochihara, T. Kadowaki, H. Minagawa, K. Hayakawa, I. Toyoshima, and C. Oshima, *Surf. Sci.* **264**, 103 (1992).

¹³S. Mizuno, H. Tochihara, and T. Kawamura, *J. Vac. Sci. Technol. A* **12**, 471 (1994).

¹⁴H. Tochihara and S. Mizuno, *Chem. Phys. Lett.* **194**, 51 (1992).

¹⁵M. A. Van Hove and S. Y. Tong, *Surface Crystallography by LEED*, Springer Series in Chemical Physics Vol. 2 (Springer, Berlin, 1979).

¹⁶S. Mizuno, and H. Tochihara, and T. Kawamura (unpublished).

¹⁷S. Mizuno and H. Tochihara (unpublished).

¹⁸N. Benazeth, C. Leonard, C. Benazeth, L. Viel, and M. Negre, *Surf. Sci.* **97**, 171 (1980).

¹⁹A. P. Janssen, R. Schoonmaker, J. A. D. Matthew, and A. Chambers, *Solid State Comm.* **14**, 1263 (1974).

²⁰X. Shi, D. Tang, D. Heskett, K.-D. Tsuei, H. Ishida, Y. Morikawa, and K. Terakura, *Phys. Rev.* **47**, 4014 (1993).

²¹D. L. Doering and S. Semancik, *Surf. Sci.* **175**, L730 (1986).

²²D. L. Doering and S. Semancik, *Surf. Sci.* **179**, 177 (1986).

²³W. R. Tyson and W. A. Miller, *Surf. Sci.* **62**, 267 (1977).

²⁴T. Matshushima and H. Asada, *J. Chem. Phys.* **85**, 1658 (1986).

²⁵T. B. Murray, L. H. Bonnet, and H. Baker, *Binary Alloy Phase Diagram* (American Society of Metals, Metals Park, OH, 1986).